JOURNAL OF NATURAL PRODUCTS

pubs.acs.org/jnp

Article

Isolinderalactone Ameliorates the Pathology of Alzheimer's Disease by Inhibiting the JNK Signaling Pathway

Li Xiong, Lingyu She, Jinfeng Sun, Xiangwei Xu, Liwei Li, Yuqing Zeng, Hao Tang, Guang Liang,* Wei Wang,* and Xia Zhao*

Cite This: https://doi.org/10.1021/acs.jnatprod.3c00894

Read Online

ACCESS | Metrics & More | Article Recommendations | Supporting Information

ABSTRACT: Neuronal cell damage is the main cause of cognitive impairment in Alzheimer's disease (AD). Multiple factors, such as amyloid deposition, tau hyperphosphorylation, and neuroinflammation, can lead to neuronal cell damage. Therefore, the development of multitarget drugs with broad neuroprotective effects may be an effective strategy for the treatment of AD. Natural products have become an important source of drug discovery because of their good pharmacological activity, multiple targets, and low toxicity. In this study, we screened a natural compound library and found that the fat-soluble sesquiterpene natural compound isolinderalactone (Iso) extracted from the dried root pieces of *Lindera aggregata* had the ability to alleviate cellular damage induced by β-amyloid-1−42 (Aβ1−42). The role and mechanism of Iso in AD have not yet been reported. Herein, we demonstrated that Iso significantly reduced the level of apoptosis in PC12 cells. Besides, Iso treatment reduced amyloid deposition, neuron apoptosis, and neuroinflammation, ultimately improving the cognitive dysfunction of APP/PS1 (APPswe/PSEN 1dE9) mice. Notably, Iso-10 mg/kg showed superior improved effects in APP/PS1 mice compared with the positive control drug donepezil-5 mg/kg. Mechanistically, the results of RNA sequencing combined with Western blots showed that Iso exerted its therapeutic effect by inhibiting the c-Jun N-terminal kinase (JNK) signaling pathway. Taken together, our findings suggest Iso is a potential drug candidate for AD therapy.

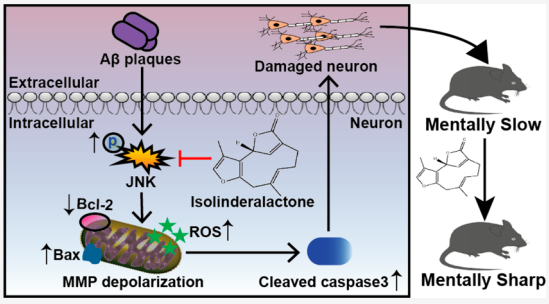

Alzheimer's disease (AD) is the most common type of dementia, clinically characterized by loss of memory. In recent years, the rising prevalence of AD has brought heavy economic and mental burdens to society and families.[1,2] Currently, there are few clinically approved drugs for the treatment of AD, and the therapeutic effect is limited. Therefore, it is urgent to develop new drug candidates with effective and low side effects for the clinical treatment of AD.[3,4]

Hippocampal neuron damage is the main cause of learning and memory disorders.[5] Multiple factors can induce neuronal damage in AD, such as senile plaques caused by Aβ amyloid deposition, neurofibrillary tangles developed by hyperphosphorylated Tau proteins, and neuroinflammation.[6] Meanwhile, neuronal damage further amplifies the pathological features of AD.[7] For example, the massive release of pro-inflammatory factors can trigger the stress response of neurons, which eventually leads to neuronal damage.[8] Damaged neurons lead to microglial activation, amplifying the inflammatory cascade.[8] The deposition of Aβ around neurons destroys the ion balance on the cell membrane surface and increases the concentration of intracellular calcium ions (Ca^{2+}) and reactive oxygen species (ROS), leading to abnormal mitochondrial membrane potential and ultimately cell death; neuron damage in turn precipitates the production of more noxious Aβ fragments.[9,10] Hyperphosphorylated tau protein dissociates from microtubule-related proteins, destroying cell membrane stability and leading to neuronal apoptosis.[11,12] In conclusion, neuronal damage interacts with other pathologies of AD, ultimately affecting spatial learning and memory in AD patients. Discovering drugs that can protect neurons from damage may be an effective strategy for treating AD.

Plant-derived small-molecule compounds have important intrinsic biological functions. Finding natural products to study as potential new drugs is one of the effective ways recognized in the field of drug research and development. During natural compound library drug screening, we discovered that isolinderalactone (Iso) conferred the best neuroprotective effect on PC12 cell injury induced by Aβ. Iso is a representative elemane-type sesquiterpene lactone mainly isolated from the rhizome of *Lindera aggregata*, which is called "Wu yao" in Chinese and is a traditional Chinese medicine herb used in the therapy of pain and inflammatory diseases. The extraction of Iso involves several procedures, including drying, pulverization, extraction, filtration, concentration,

Received: September 25, 2023
Revised: November 22, 2023
Accepted: November 23, 2023

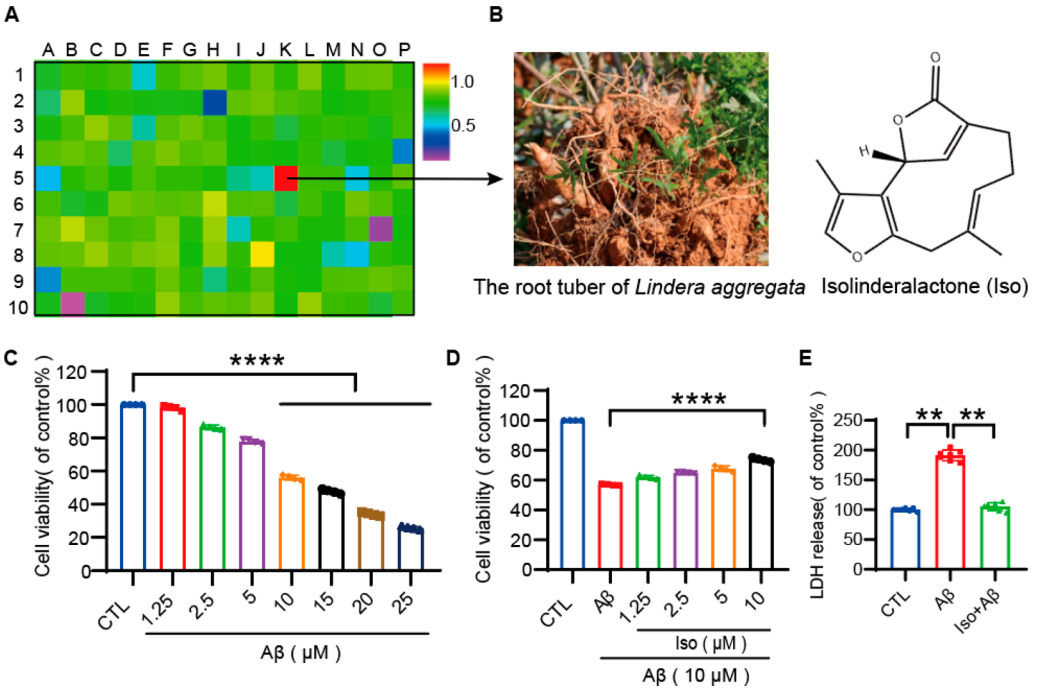

Figure 1. Iso attenuates Aβ1−42-induced injury in PC12 cells. (A) We screened 160 compounds for their protective effects against Aβ1−42-induced injury in PC12 cells; Iso showed the best results. (B) Chemical structure of Iso. (C) Concentration screening of Aβ1−42. PC12 cells were stimulated with different concentrations of Aβ1−42 for 24 h, followed by MTT assay. (D) PC12 cells were pretreated with different doses of Iso for 3 h and then exposed to Aβ1−42 for 24 h. Iso attenuates Aβ1−42-induced injury in PC12 cells. Cell viability was measured using the MTT assay. (E) Cells were pretreated with 10 μM Iso for 3 h and then induced for an additional 24 h with or without 10 μM Aβ1−42. Cell membrane damage was measured by LDH release assay. $^{*}P < 0.05$ or $^{**}P < 0.01$, or $^{***}P < 0.001$.

crystallization, and purification. Iso exerts various physiological activities, such as antioxidant and anti-inflammatory actions, which are closely related to AD pathogenesis.[13]

In this study, we evaluated the therapeutic effect of Iso in AD. RNA sequencing combined with Western blots was used to elucidate the potential mechanism of Iso in AD. Our results showed that Iso was more effective than the marketed drug donepezil in APP/PS1 mice and may be considered as a potential candidate for AD intervention.

RESULTS

Iso Attenuates Aβ1−42-Induced Cell Damage in PC12 Cells. Accumulation of Aβ is considered as an early occurrence in AD pathogenesis.[14,15] Aβ1−42, a well-established model of neuronal cell injury in AD, has been implicated in eliciting various cytotoxic responses, including oxidative stress, neuroinflammation, and mitochondrial dysfunction. In the current research, we performed a screening process to identify the most potent small-molecule compounds for alleviating neuronal damage. A library comprising 160 natural compounds (Table S1) was employed for this purpose. Initially, PC12 cells were subjected to pretreatment with different compounds (10 μM) for 2 h, subsequently accompanied by stimulation with 10 μM Aβ1−42 for 24 h. Then, cell viability was detected by using an MTT assay. Remarkably, among the tested compounds, Iso displayed the most pronounced neuroprotective effect against Aβ1−42-induced neuronal cell injury, as depicted in Figure 1A (Figure 1A). Iso has a sesquiterpene structure (Figure 1B) and a wide range of physiological activities, such as anti-inflammatory, antioxidant, and antibacterial activities. To find the appropriate Aβ1−42 modeling concentration, we stimulated PC12 cells with diverse concentrations of Aβ for 24 h and performed the MTT assay. According to the results, Aβ1−42-10 μM was selected as the subsequent experimental concentration (Figure 1C). Then, we examined the protective effect of Iso on the Aβ1−42-induced neuronal injury. PC12 cells were subjected to pretreatment with different concentrations of Iso for 3 h and subsequently exposed to Aβ1−42 (10 μM) for 24 h. The MTT assay results indicated that Iso pretreatment significantly reduced Aβ1−42-induced PC12 cell damage (Figure 1D). Subsequently, we measured the amount of lactate dehydrogenase (LDH) in the cell supernatant. These results implied that Iso pretreatment markedly reduced the level of Aβ1−42-induced LDH release (Figure 1E).

Iso Reduces Aβ1−42-Induced Neurotoxicity in PC12 Cells. To further determine the protective effect of Iso on Aβ1−42-induced cell damage, we performed flow cytometry and found that Iso at a concentration of 10 μM could reduce Aβ1−42-induced neuronal damage (Figure 2A and 2B). Similarly, the Iso pretreatment significantly decreased the level of cleaved caspase-3 in PC12 cells (Figure 2C). Furthermore, Western blot results showed increased Bax expression and intracellular levels of caspase-3 activation and decreased Bcl2 levels in Aβ1−42-stimulated PC12 cells, whereas Iso pretreatment reversed these changes (Figure 2D and 2E). The above results indicated that Iso pretreatment could attenuate Aβ1−42-induced apoptosis in PC12 cells. Aβ1−42 can increase ROS levels and perturb mitochondrial membrane potential in PC12 cells.[16,17] We found that intracellular ROS levels were significantly reduced, and mitochondrial membrane potential was restored after Iso pretreatment (Figure 2F and 2G).

https://doi.org/10.1021/acs.jnatprod.3c00894
J. Nat. Prod. XXXX, XXX, XXX−XXX

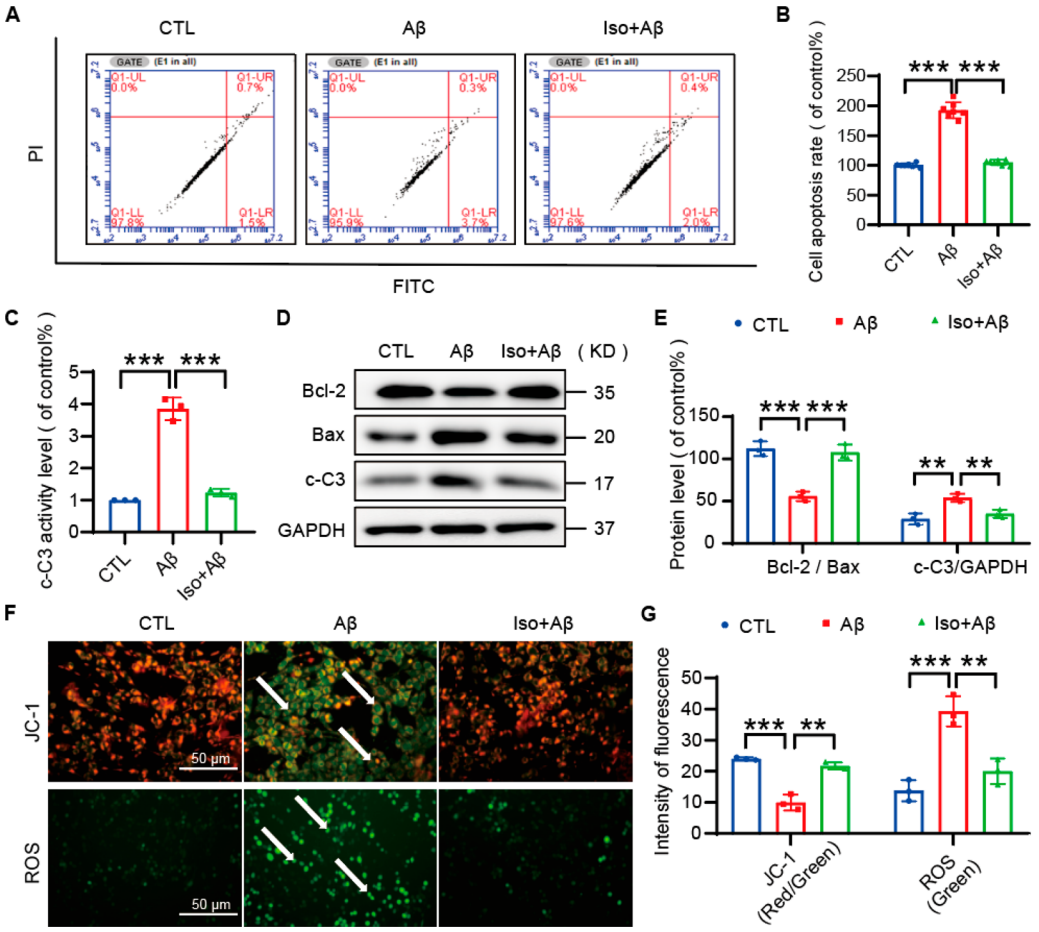

Figure 2. Iso reduces Aβ1−42-induced apoptosis in PC12 cells. Cells were pretreated with 10 μM Iso for 3 h and then stimulated for an additional 24 h with 10 μM Aβ1−42. (A) Apoptosis was measured by flow cytometry. (B) Quantitative analysis of (A). (C) Activity of cleaved caspase-3. (D) Western blot analysis of Bax, cleaved caspase-3, and Bcl-2 in PC12 cells. (E) Quantitative data of Bcl-2/Bax ratio and cleaved caspase-3 blot intensity determined by ImageJ software. (F) Representative images of JC-1 and ROS staining in PC12. (G) Quantitative analysis of (F). $^{*}P < 0.05$ or $^{**}P < 0.01$, or $^{***}P < 0.001$.

Iso Protects Neuronal Cells from Damage by Inhibiting the JNK Signaling Pathway. To explore the mechanism by which Iso protects PC12 cells, we performed RNA sequencing. PC12 cells were divided into three groups: CTL, Aβ, and Iso+Aβ. After drug treatment, the samples were collected into Trizol and sent to a company for sequencing. After analysis, 2003 significantly changed genes were selected (Figure 3A). Subsequently, a KEGG pathway enrichment analysis was performed on the identified set of 2003 genes. Results revealed that these genes were primarily associated with 19 signal transduction pathways. Notably, the mitogen-activated protein kinase (MAPK) signaling pathway ranked first (Figure 3B). MAPKs are recognized as pivotal mediators of signal transmission from the cell membrane to the nucleus, playing critical roles in modulating cellular processes such as proliferation, differentiation, and apoptosis.[18] In nerve cells, three MAPKs are known to be closely linked to cell growth and death, namely, extracellular regulated protein kinases (ERK), p38, and JNK.[19] We analyzed the changes in these three kinases by Western blotting, and the results showed that the JNK pathway was most affected by Iso treatment. Iso pretreatment significantly decreased the level of p-JNK, but had no significant effect on ERK and P38MAPK (Figure 3C and 3D), suggesting that Iso may play a protective role by inhibiting JNK phosphorylation. To verify this result, we pretreated with the JNK inhibitor SP600125, and the MTT assay found that the cell viability of the three groups (SP600125+Aβ, Iso+Aβ, and SP600125+Iso+Aβ) was significantly increased compared with that of the Aβ group. However, there were no significant differences among the three groups (Figure 3E). Similarly, according to the Western blot analysis, there were no significant alterations observed in the Bcl2/Bax ratio and level of cleaved caspase-3 protein among groups 3, 4, and 5 subsequent to the addition of JNK-specific inhibitors (Figure 3F and 3G). These observations indicated that Iso might exert neuroprotective effects by suppressing the JNK signaling pathway, thereby safeguarding neuronal cells against injury.

Iso Ameliorates Learning and Memory Deficits in APP/PS1Mice. We next performed animal experiments to determine the potential therapeutic effect of Iso in AD. We selected 10-month-old APP/PS1 transgenic mice, injected Iso intraperitoneally for 1 month, and then performed animal behavior tests to evaluate cognitive function and detect related pathology (Figure 4A and 4B). First, we performed the novel object recognition test, and the mouse movement trajectory graph showed that the APP/PS1 model group exhibited lower exploratory behavior and average movement speed than the WT group on day 1, but Iso treatment improved these changes. After the new object was changed on day 2, it was

https://doi.org/10.1021/acs.jnatprod.3c00894
J. Nat. Prod. XXXX, XXX, XXX−XXX

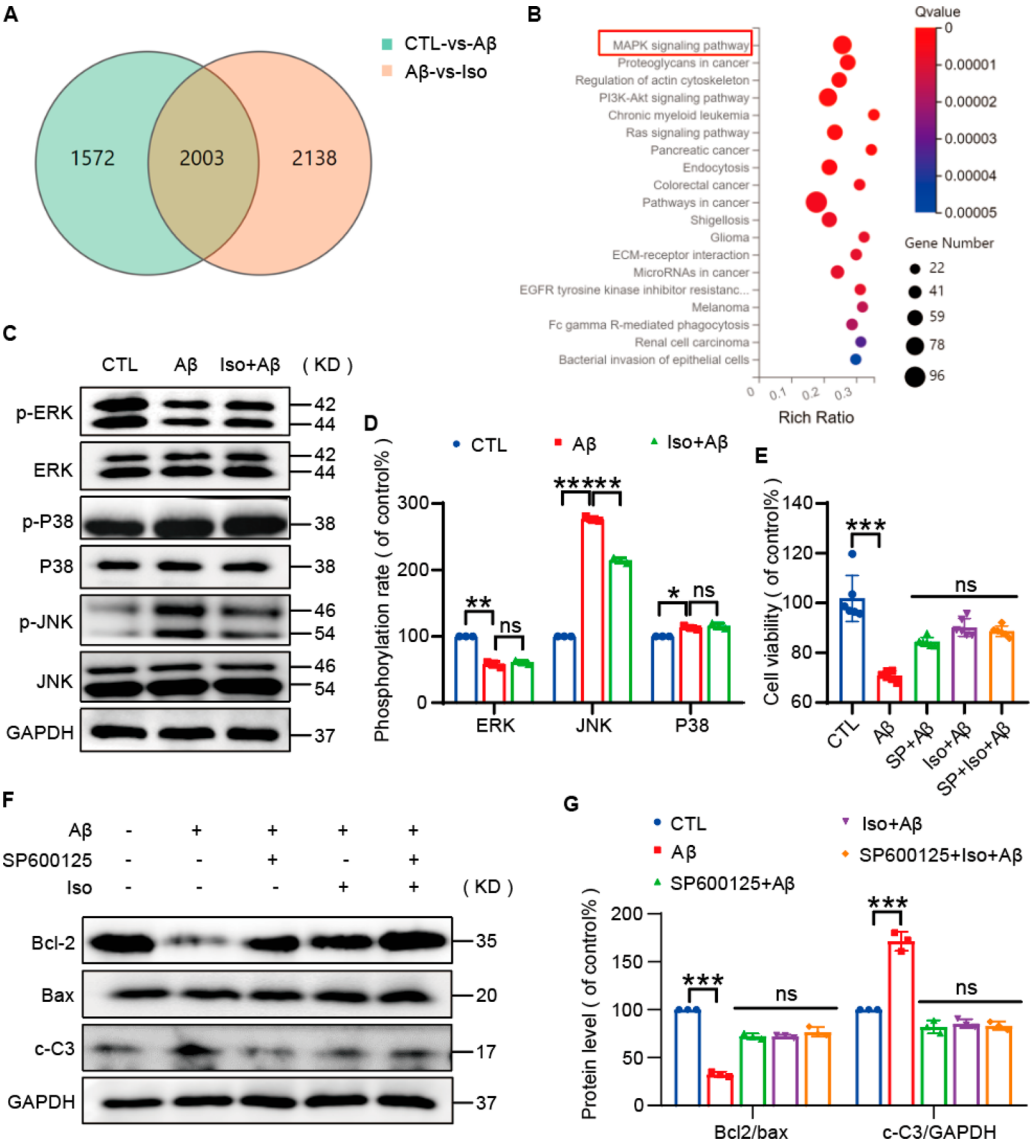

Figure 3. Iso reduces neuronal cell damage by inhibiting JNK. PC12 cells were pretreated with or without 1.25 μM SP600125 for 0.5 h. PC12 cells were then protected with 10 μM Iso for 3 h and then exposed to 10 μM Aβ for 24 h. (A) Number of significant genes in RNA-Seq. (B) KEGG enrichment analysis of 2003 significant gene signaling pathways. (C) Western blot results of the three main enzymes of MAPK. (D) Quantitative statistics of the blot intensity of (C) using ImageJ software. (E) Cell viability was measured using the MTT assay. (F) Western blot analysis of Bax, cleaved caspase-3, and Bcl-2 in PC12 cells. (G) Quantitative data of blot intensities of corresponding proteins determined by ImageJ software. *P < 0.05 or **P < 0.01, or ***P < 0.001.

found that high-dose Iso treatment greatly enhanced the exploration of the novel object by the mice, and the pretreated mice explored the novel object at high frequency and for a long time (Figure 4C−4F). The MWM test provided additional evidence supporting the beneficial effects of Iso on learning and memory. Analysis of the results revealed that APP/PS1 mice exhibited prolonged escape latency, reduced platform crossings, and decreased time spent in the target quadrant. In contrast, treatment with a high dose of Iso or donepezil substantially ameliorated these parameters and enhanced spatial memory in APP/PS1 mice, with Iso at a dose of 10 mg/kg exhibiting superior improved effects compared to the positive control drug donepezil-5 mg/kg (Figure 5A−5H). Taken together, these outcomes strongly suggested that Iso possessed the capability to ameliorate cognitive deficits in APP/PS1 mice.

Iso Alleviates AD Pathology of APP/PS1 Mice. Aβ plaques and neuroinflammation are the two main pathological features of AD.[20] Immunofluorescence staining results showed that treatment with Iso or donepezil reduced the level of Aβ plaque deposition and glial cell aggregation in the hippocampus of APP/PS1 mice. Importantly, higher doses of Iso showed better therapeutic effects (Figure 6A−6D). Next, we selected the hippocampal tissue homogenate of mice to perform Western blot experiments. The findings demonstrated that treatment with Iso resulted in a significant reduction in the level of APP/β-amyloid, concomitant with a significant increase in the levels of synapse-associated proteins, including postsynaptic density protein 95 (PSD95) and microtubule-associated protein 2 (Map2) (Figure 6E and 6F). Interestingly, Iso showed a better improved effect at a dose of 10 mg/kg in comparison to donepezil-5 mg/kg in promoting the expression of synapse-associated proteins.

https://doi.org/10.1021/acs.jnatprod.3c00894
J. Nat. Prod. XXXX, XXX, XXX−XXX

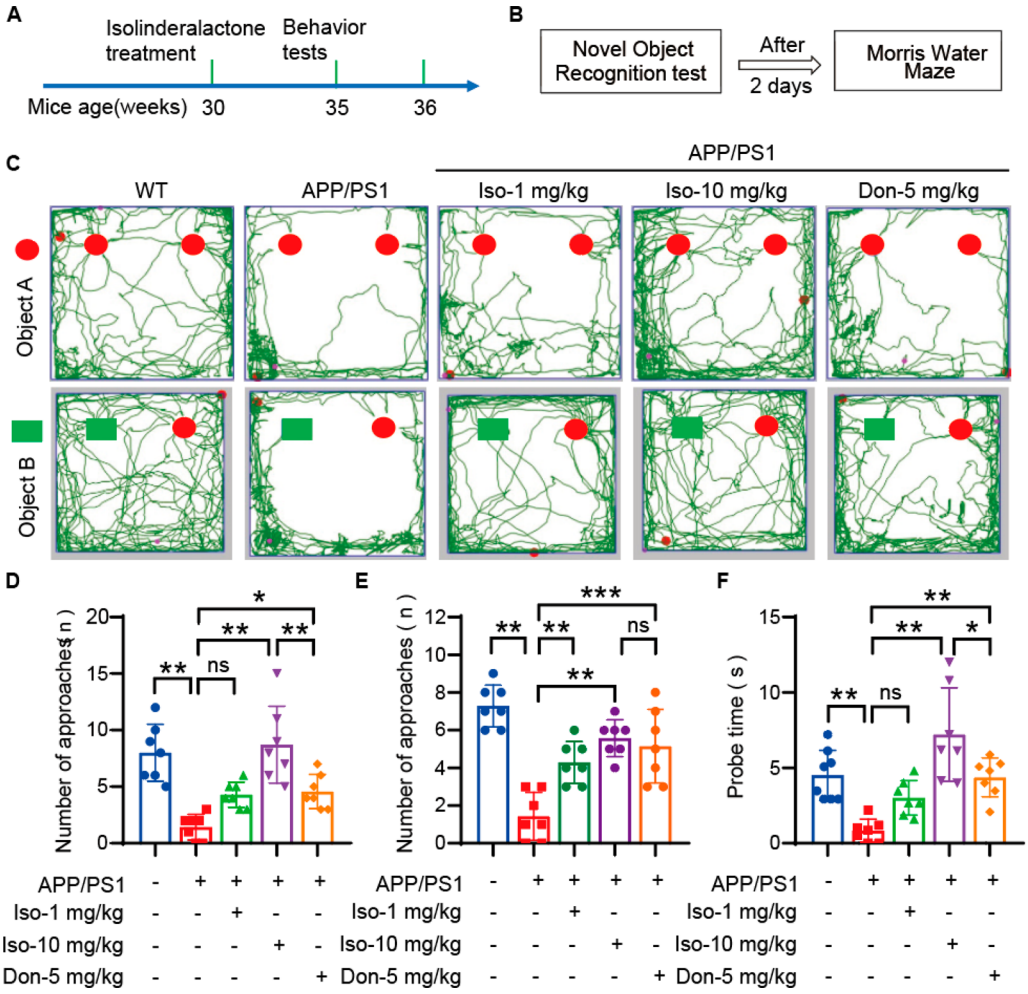

Figure 4. Iso improves the novel object exploration of APP/PS1 mice. APP/PS1 mice were administered Iso intraperitoneally once daily for 30 consecutive days at low (1 mg/kg) and high (10 mg/kg) doses. (A) Timeline of animal experiment. (B) Behavioral tests performed in APP/PS1 mice. (C) Representative images of the novel object recognition paradigm. (D) Preference for objects on the first day of the novel object recognition test. (E) The number of approaches to the novel object. (F) Probe time of the novel object approaches in the new object recognition test. $^{*}P < 0.05$ or $^{**}P < 0.01$, or $^{***}P < 0.001$ versus the APP/PS1 group.

Iso Treatment Reduces Neuronal Apoptosis in APP/PS1Mice. Neuronal apoptosis can lead to neuronal loss, impaired synapse formation, and neuroinflammation.[21] Reducing neuronal apoptosis can significantly delay the onset and progression of AD.[22] We first performed tissue immunofluorescence. The results showed that Iso treatment could reduce neuronal apoptosis in the cortex and hippocampus (Figure 7A−7C). Neuronal apoptosis is closely related to oxidative stress. Therefore, we examined the levels of SOD and MDA in mouse hippocampal homogenates. Iso or donepezil treatment significantly increased the SOD content and decreased MDA levels in the hippocampus of APP/PS1 mice (Figure 7D and 7E). Subsequently, we detected the expression of apoptosis-related proteins in the mouse hippocampus using Western blot. Iso treatment significantly increased Bcl2 levels, decreased Bax expression, and decreased caspase-3 activation compared to APP/PS1 mice (Figure 7F−7H). Similarly, we also detected the expression of p-JNK. In comparison to the APP/PS1 group, p-JNK levels were significantly suppressed in the Iso-treated group (Figure 7I and 7J). This finding provides further evidence that Iso protects neurons from apoptosis by inhibiting JNK phosphorylation.

DISCUSSION

In the past decades, researchers have been working on synthesizing new compounds for AD treatment, and little progress has been made. However, failures do not mean that we should give up AD drug development. On the contrary, we might be able to get a new direction—natural products. In recent years, many studies on the use of natural products in the treatment of AD have emerged. Natural products offer relatively low toxicity, reducing the risk of side effects in the body. In addition, natural products come from various organisms in nature, and therefore, the development of natural products can incorporate protection of the ecological environment and promote the development of the pharmaceutical industry.

In this study, we verified that Iso pretreatment reduced Aβ1−42-induced apoptosis, restored mitochondrial membrane potential disorder, and decreased intracellular ROS levels in PC12 cells. In APP/PS1 mice, Iso treatment reduced Aβ plaque deposition and impaired synaptic plasticity and glial cell activation, which in turn ameliorated cognitive deficits in model mice. Notably, Iso at a dose of 10 mg/kg had improved properties compared to the positive drug donepezil-5 mg/kg. Mechanistically, the results of RNA-sequencing and SP600125

https://doi.org/10.1021/acs.jnatprod.3c00894
J. Nat. Prod. XXXX, XXX, XXX−XXX

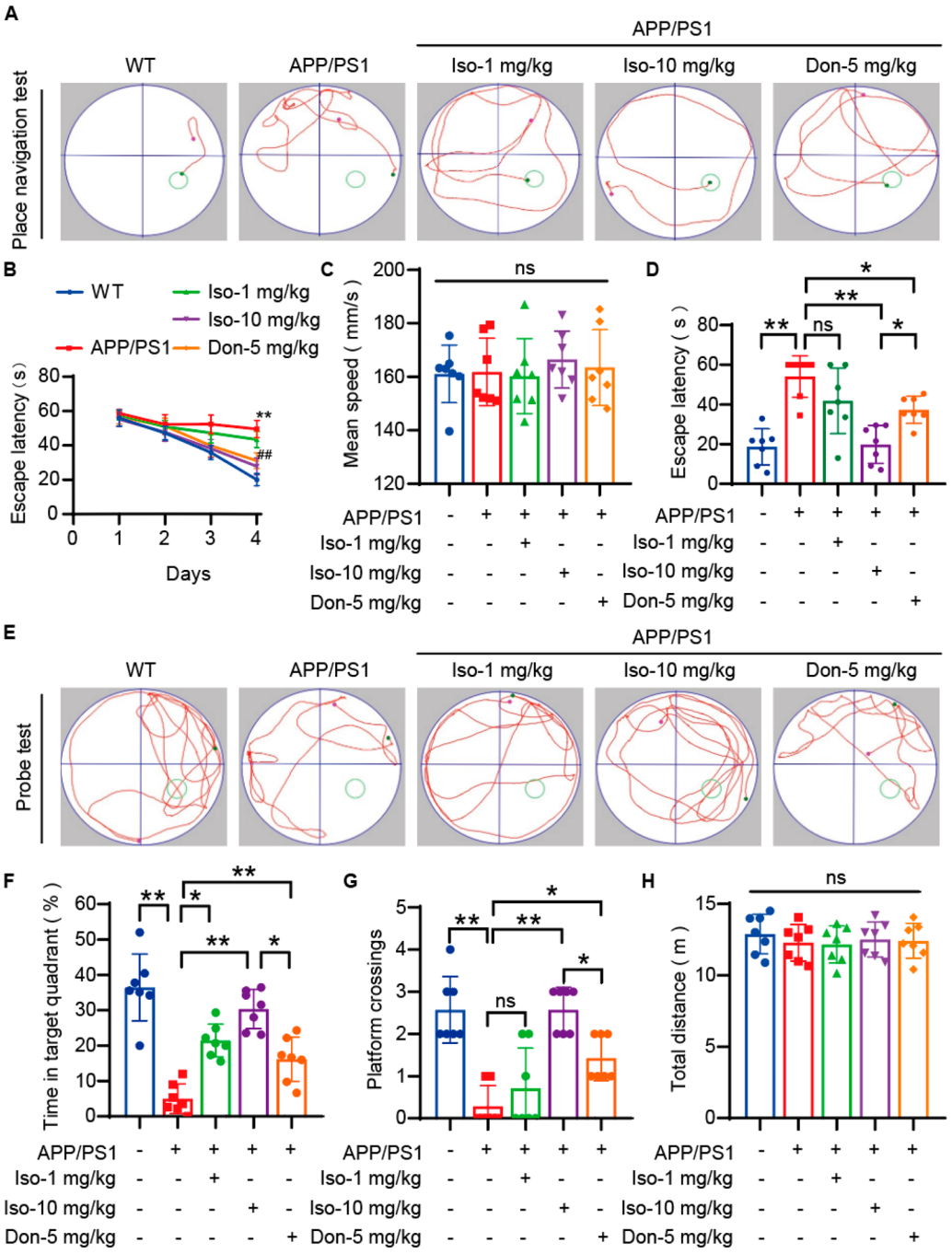

Figure 5. Iso ameliorates learning and memory deficits in APP/PS1 mice. (A) The representative swimming trace in a probe trial of the Morris water maze test on day 5. (B) Escape latency of mice on days 1−5. (C) Mean swimming speed of mice. (D) The time needed to find the hidden platform (escape latency) on day 5. (E) The representative swimming trace in the probe trial without the hidden platform of the Morris water maze test on day 6. (F) Time spent in the target quadrant where the platform had been located for the first 5 days. (G) The average number of platform crossings for each group of mice within 60 s on day 6. (H) Total distance of mice. $^{*}P < 0.05$ or $^{**}P < 0.01$, or $^{***}P < 0.001$ versus the WT group; $^{\#}P < 0.05$ or $^{\#\#}P < 0.01$ versus the APP/PS1 group.

pretreatment both confirmed that Iso reduced neuronal damage by inhibiting the JNK signaling pathway.

Iso, a traditional Chinese medicine ingredient, is one of the principal active components of *L. aggregata* and has various functions under pathological conditions. Kwak et al. have suggested that Iso potentiates the susceptibility of oxaliplatin-resistant colorectal cancer cells via the JNK/p38 MAPK signaling pathway,[23] implying the potential role of Iso in modulating the JNK signaling pathway. This mechanism was also proven in our experiment. Compared with some other natural products, Iso has beneficial properties. Penetration of the blood brain barrier (BBB) has always been a difficult problem in the development of central nervous system (CNS) drugs. However, according to the database (TCMSP), the BBB penetration ratio of Iso was 0.96, predicting efficient access to the CNS. Besides, Hwa Park et al. have reported that Iso suppresses human glioblastoma growth and angiogenic activity in a 3D microfluidic chip and *in vivo* mouse models, indicating

https://doi.org/10.1021/acs.jnatprod.3c00894
J. Nat. Prod. XXXX, XXX, XXX−XXX

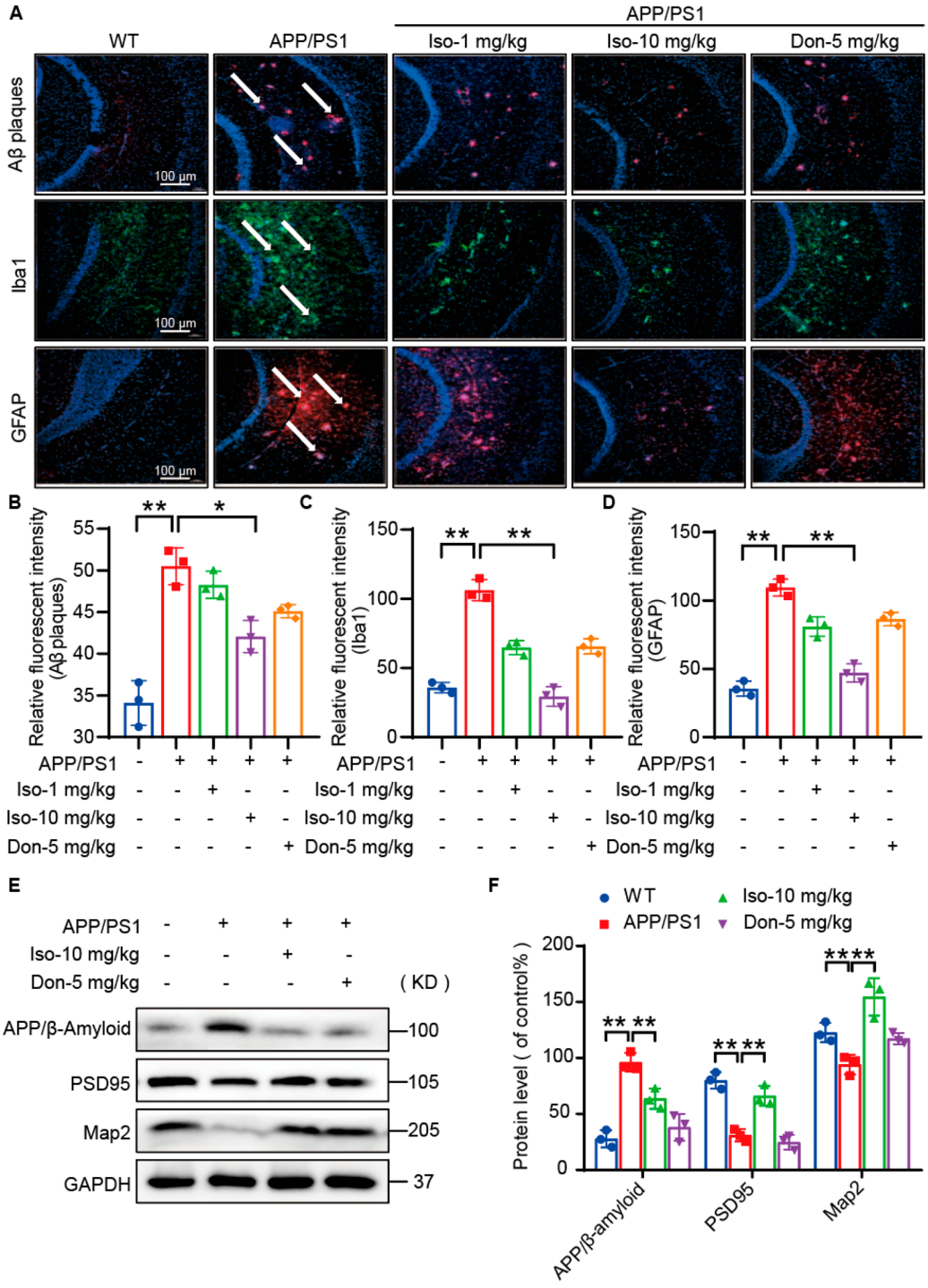

Figure 6. Iso alleviates AD pathology in APP/PS1 mice. (A) Representative immunofluorescence images of the hippocampal CA1 region of five groups of mice (10-month-old). Scale bar: 100 μm. (B–D) Quantitative analysis of (A). (E) Representative Western blotting analysis of APP, Map2, and PSD95 in the hippocampal homogenate. (F) Quantitative data of blot intensities of corresponding proteins were determined by ImageJ software in plane A. *P < 0.05 or **P < 0.01, or ***P < 0.001.

the ability of Iso to cross the BBB.[24] The role of ginseng in AD has been extensively reported.[25−27] Compared with ginseng, the raw material of Iso is less expensive. Last but not the least, modern pharmacological studies have shown that some single herbs and their effective parts have excellent therapeutic effects on AD, such as *Polygala tenuifolia*, *Uncaria rhynchophylla*, and polysaccharides of *Schisandra chinensis fructus*.[28−30] Conversely, Iso, as a single compound extracted from the root of *L. aggregata*, is more conducive for clarifying its target of action, predicting side effects, and facilitating better clinical evaluation than a complex mixture.

JNK is a key target recently shown to be involved in AD pathology. Neuronal damage is closely related to the JNK-mediated signaling pathway.[31] For example, microRNA-326 inhibits the JNK signaling pathway by targeting VAV1 to reduce neuronal apoptosis;[32] VB-037 reduces Aβ aggregation and neuronal apoptosis by inhibiting JNK phosphorylation;[33] vitegnoside mitigates neuronal injury, mitochondrial apoptosis,

https://doi.org/10.1021/acs.jnatprod.3c00894
J. Nat. Prod. XXXX, XXX, XXX−XXX

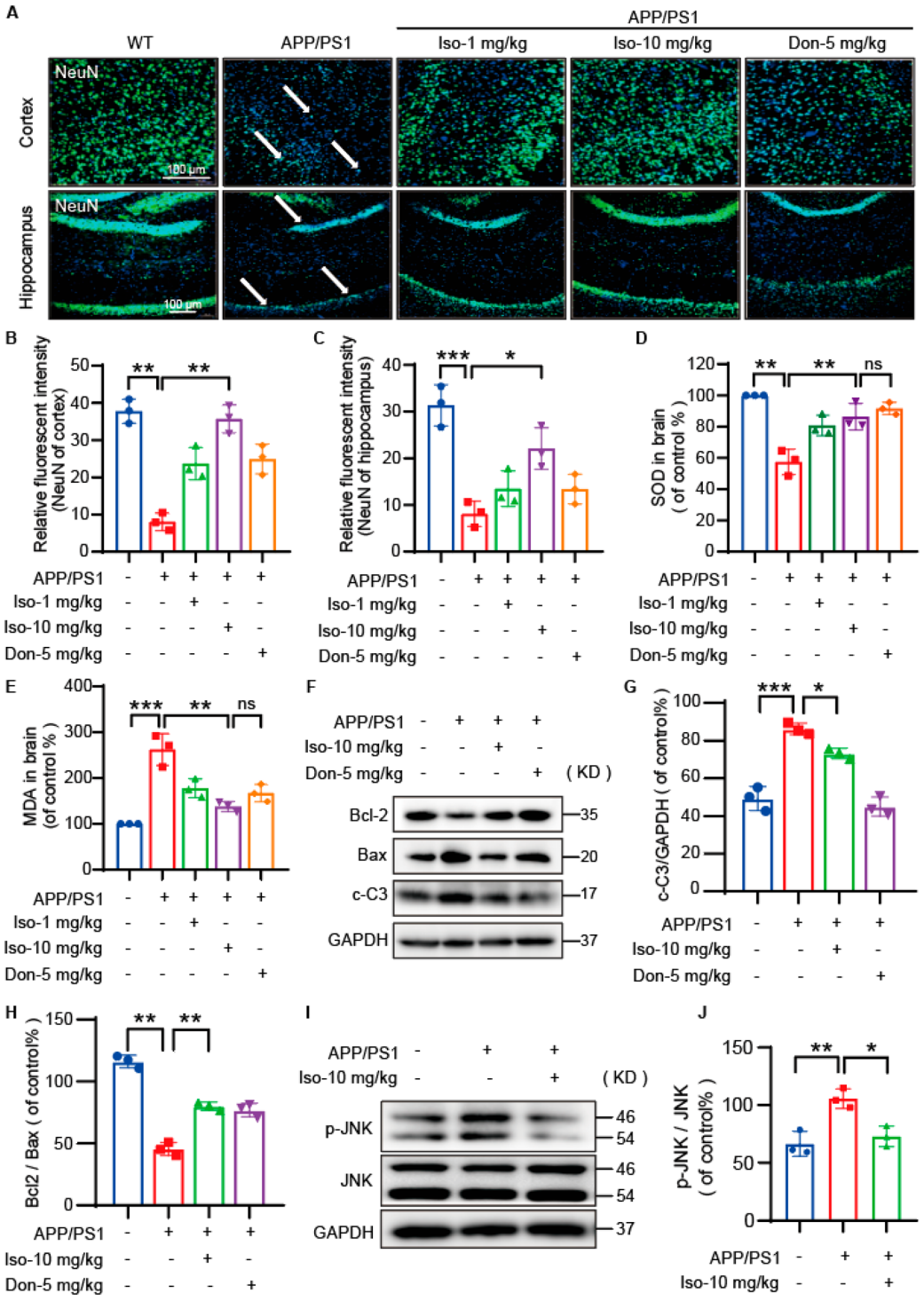

Figure 7. Iso treatment reduces neuronal apoptosis in APP/PS1 mice. (A) Representative images of neuronal immunofluorescence in the cortex and hippocampal regions of five groups of mice (10-month-old). (B, C) Quantitative analysis of (A). (D, E) Hippocampal levels of SOD and MDA levels were determined using biochemical kits, respectively. (F) Representative Western blot analysis of Bax, Bcl-2, and cleaved caspase-3 in the hippocampal homogenate. (G, H) Quantitative analysis of (F). (I) Expression levels of JNK and p-JNK were measured using Western blotting. (J) Quantitative analysis of (I). $^{*}P < 0.05$ or $^{**}P < 0.01$, or $^{***}P < 0.001$.

and inflammation in an Alzheimer's disease cell model via the p38 MAPK/JNK pathway.[34] Under normal conditions, JNK mainly exists in the cytoplasm. Once cells are subjected to a harmful stimulation, JNK phosphorylation increases. Phosphorylated JNK can enter the nucleus to promote the transcription of apoptosis-related factors and acts directly on mitochondria, down-regulating the expression of Bcl2 and up-regulating that of Bax while activating caspase-3. In addition, p-JNK can induce neuronal apoptosis by stimulating the FasL-Fas pathway and other mechanisms. Herein, Iso mainly functioned by inhibiting JNK phosphorylation, as confirmed by cellular RNA-sequencing technology and the specific JNK inhibitor SP600125. We subjected the 2003 genes involved in changes before and after stimulation to KEGG for pathway

https://doi.org/10.1021/acs.jnatprod.3c00894
J. Nat. Prod. XXXX, XXX, XXX−XXX

analysis and found that the MAPK signal transduction pathway ranked first. Therefore, we performed a Western blot assay and found that Iso exhibited the most notable inhibitory effect on JNK. Moreover, Iso did not afford neuroprotection when PC12 cells were pretreated with SP600125. Based on the WB results, we concluded that Iso could markedly inhibit JNK phosphorylation at both *in vitro* and *in vivo* levels. It should be noted that the positive control donepezil, as an acetylcholinesterase inhibitor, has a mechanism of action different from Iso. Donepezil was chosen as the positive control, as it is an FDA-approved drug that can currently be used to treat mild and moderate AD. The current study seems to imply that we should search for new targets in order to achieve improved therapeutic effects on AD, and JNK might be a valuable target. However, whether Iso exerts direct or indirect inhibition of JNK phosphorylation remains to be explored.

Our results demonstrated the significant protective effects of Iso against Aβ1−42-induced PC12 cell damage as well as its ability to attenuate AD pathology and cognitive deficits in a mouse model of AD (APP/PS1 mice). The RNA sequencing results revealed that Iso exerted its therapeutic effects through the inhibition of JNK phosphorylation. Moreover, Iso at 10 mg/kg had improved properties compared to that of 5 mg/kg-donepezil. Collectively, these results highlight the potential of Iso as a novel pharmaceutical candidate for the treatment of AD.

EXPERIMENTAL SECTION

Reagents. Isolinderalactone (purity: HPLC ≥ 98%) was obtained from MeilunBio. Fetal bovine serum (FBS) and 0.25% trypsin were procured from Life Technologies and Calbiochem, respectively. Bovine serum albumin (BSA), dimethyl sulfoxide (DMSO), and Dulbecco's modified Eagle's medium (DMEM) were purchased from Sigma. The phosphatase inhibitor cocktail was purchased from Fisher Scientific. The Annexin V-FITC/PI apoptosis detection kit was purchased from BD Biosciences. Penicillin/streptomycin was obtained from Gibco. Polyvinylidene difluoride (PVDF) membranes were purchased from Bio-Rad. Caspase-3 activity assay kit, superoxide dismutase (SOD) assay kit, lipid peroxidation malonaldehyde (MDA) assay kit, MTT powder, JC-1 kit, DAPI dye, DCFH-DA reagent, and RIPA lysis buffer were all obtained from the Beyotime Institute of Biotechnology. Aβ1−42 (PA4391), NH2-DAEFRHDSGYEVHHQKLVFFAEDVGSNKGAIIGLMVGGVVIA−COOH ($C_{203}H_{311}N_{55}O_{60}S$; molecular mass: 4514.10), was obtained from Ontores Biotechnologies. The antibodies used and their sources are presented in Table 1.

Cell Culture and Treatments. PC12 cells were cultured in DMEM supplemented with 10% FBS and 0.1% penicillin/streptomycin in 75 cm^2 dishes. Cells were cultured at 37 °C under a humidified atmosphere containing 5% CO_2. The medium was refreshed every 2 to 3 days and subcultured with 0.25% trypsin when the cells reached approximately 80−90% confluency. After trypsin digestion, cells were subjected to centrifugation at 1000 rpm for 3 min and subsequently reconstituted in fresh medium. Only adherent cell cultures were utilized in all experimental procedures.

Aβ Oligomer Preparation. Establishing a suitable model is crucial for studying the pathological mechanism of AD. Aβ accumulation is a precedent occurrence in AD progression, which induces a variety of complex pathological changes, such as Aβ sedimentation, neuronal loss, and cognitive dysfunction in learning and memory.[35] What is more, Aβ oligomers have the strongest neurotoxic effects. It is generally accepted that Aβ1−42 is the most aggregate-prone of all Aβ fragments.[36] Therefore, we chose the Aβ1−42 oligomer-induced cell injury model. In this study, Aβ1−42 was dissolved and stocked at a concentration of 10 mM in sterile DMSO. As previously elucidated, Aβ1−42 was incubated at a temperature of 37 °C for a time period of 7 days preceding use in order to form aggregates.[36−38] When used in cell experiments, the high concentration of oligomers was further diluted with a cell culture medium to a suitable concentration.

Table 1. Antibody Information

antibody	cat. no.	source	dilution
PSD95	2507	CST[a]	WB[b]:1:1000
MAP2	4542	CST	WB:1:1000
Iba1	17198	CST	IF[c]:1:100
GFAP	3670	CST	IF:1:200
APP/β-Amyloid	2450	CST	IF:1:200
JNK	9252	CST	WB:1:1000
P-JNK(Thr183/Thr185)	4668	CST	WB:1:1000
ERK	4696	CST	WB:1:1000
P-ERK (Thr202/Thr204)	4370	CST	WB:1:1000
P38MAPK	8690	CST	WB:1:1000
P-P38MAPK(Thr180/Thr182)	4511	CST	WB:1:1000
Bax	2774	CST	WB:1:1000
Bcl2	15071	CST	WB:1:1000
NeuN	24307	CST	IF:1:200
cleaved caspase-3	9661	CST	WB:1:1000
GAPDH	AF0006	Beyotime	WB:1:2000
anti-rabbit IgG HRP	A0208	Beyotime	WB:1:2000
anti-mouse IgG HRP	A0216	Beyotime	WB:1:2000
Alexa Fluor 594	8889	CST	IF: 1:500
Alexa Fluor 488	4412	CST	IF: 1:500

[a]CST: Cell Signaling Technology. [b]WB: Western blot. [c]IF: immunofluorescence.

MTT Assay. Cell viability was assessed by utilizing the MTT assay in accordance with the reagent specification as specified by the manufacturer. Briefly, cells were seeded in 96-well plates at a density of 5 × 10^3 cells/well. After drug treatment, the cells were incubated with MTT (0.5 mg/mL) for 3−4 h. Subsequently, MTT was discarded, and 100 μL of DMSO was added to dissociate the sky-blue formazan crystals produced by living cells. Optical density was recorded at 570 nm by using a microplate spectrophotometer (SpectraMax 250, Molecular Devices). Cell viability was determined as a percentage relative to that of the control group (CTL).

Flow Cytometry. PC12 cells were seeded into six-well plates at a density of 5 × 10^5 cells per well. After the corresponding drug treatment, all groups of cells were collected and centrifuged at 1000 rpm for 5 min. Cells were then washed twice with cold 1× PBS and resuspended in binding buffer containing FITC (5 μL). The cells were incubated for 30−40 min at room temperature in the dark. Next, the cells were centrifuged again at 1000 rpm for 3 min and stained with propidium iodide (PI) (10 μL) for 5 min in the dark. Apoptotic cells were quantified by flow cytometry.

Caspase-3 Activity Assay. The caspase-3 activity was assessed by utilizing a caspase-3 activity assay kit (C1115, Beyotime). Following a 24 h management, cells were detached using 0.25% trypsin for 1 min at 37 °C and garnered by centrifugation at 500*g* for 5 min at 4 °C. The clarified medium was discarded, and cells were purified with 1× PBS. Subsequently, 100 μL of lysis buffer was added to meet the requirements of 2 million cells according to the manufacturer's protocol. Cells were lysed on ice for 15 min and centrifuged at 12000*g* for 15 min at 4 °C. Then, 40 μL of detection buffer and 10 μL of Ac-DEVD-pNA (2 mM) were combined with 50 μL of each sample. The resulting mixtures were gently mixed, avoiding bubble formation, and incubated for 60−120 min at 37 °C. The levels of *p*-nitroaniline (pNA) were determined by measuring the absorbance at 405 nm using an Infinite M200 PRO multimode microplate reader. Caspase-3 activity was expressed relative to that of the standard group.

Western Blotting (WB). Proteins from cultured cells and brain homogenates were extracted with an RIPA buffer. Then, the concentration of proteins was detected by using a BCA assay kit (Thermo Fisher, 23225). Subsequent to electrophoresis, the proteins

https://doi.org/10.1021/acs.jnatprod.3c00894
J. Nat. Prod. XXXX, XXX, XXX−XXX

were transferred onto PVDF membranes with a pore size of 0.22 μm for a duration of 90 min. The PVDF membranes were then subjected to blocking with 5% BSA in TBST (Tris-buffered saline containing 0.05% Tween 20) for 2 h at room temperature. Following blocking, the membranes underwent overnight incubation at 4 °C with primary antibodies at a dilution of 1:1000. The next day, the primary antibodies were washed three times with 1× TBST, and subsequently membranes underwent a 2 h incubation with a horseradish peroxidase (HRP)-conjugated secondary antibody at room temperature. Specific protein bands were visualized by using a Bio-Rad Gel Doc XR documentation system. After exposure to a bio-chemiluminescence reagent, the band intensities were quantified using the ImageJ software (U.S. National Institutes of Health).

Measurement of Mitochondrial Membrane Potential (Δψm). Changes in the mitochondrial membrane potential (Δψm) of cells were measured using a JC-1 assay kit (Beyotime, C2006) following the procedure provided by the manufacturer. After appropriate intervention, cells were incubated with 1× JC-1 reagent (10 μg/mL, FBS-free medium) for 30 min at 37 °C and then washed twice with 1× PBS solution. Measurements of red fluorescence emission (excitation: 560 nm; emission: 595 nm) and green fluorescence (excitation: 485 nm; emission: 535 nm) were quantified using an Infinite M200 PRO multimode microplate reader. Δψm was determined by calculating the ratio of JC-1 red to green fluorescence intensities. All data were normalized to those obtained from the control group.

Measurement of ROS. Intracellular ROS levels were determined using the fluorescent probe DCFH-DA (Beyotime, S0033S) according to the manufacturer's instructions. After drug treatment, cells were incubated with the DCFH-DA reagent (10 μM in FBS-free DMEM) for 30 min in the dark and washed twice with a 1× PBS solution. Fluorescence intensity was quantified using an Infinite M200 PRO multimode microplate with the excitation set at 488 nm and emission set at 525 nm.

RNA-seq Analysis. RNA sequencing was conducted by the Wuhan Huada Gene Technology Company. Triplicate RNA samples from each experimental group were prepared to undergo RNA-Seq analysis. The acquired sequencing data were subjected to filtration using SOAPnuke (v1.5.2). High-quality reads were aligned to the reference genome by employing HISAT2 (v2.0.4). Fusion genes were detected using Ericscript (v0.5.5), and differentially spliced genes (DSGs) were examined with rMATS (V3.2.5). Clean reads were mapped to a gene set database specific to the organism under investigation comprising both known and novel coding transcripts. This database was established by BGI (Beijing Genomic Institute in Shenzhen), and the alignment was executed using Bowtie2 (v2.2.5). Gene expression levels were quantified using RSEM (v1.2.12). A heatmap was created with pheatmap (v1.0.8), according to gene expression patterns across various samples. Differential expression analysis was conducted utilizing DESeq2 (v1.4.5), with a significance threshold of Q value ≤ 0.05.

Animals and Treatment. APP/PS1 (APPswe/PSEN 1dE9) double-transgenic mice (n = 40) were sourced from the Jackson Laboratory and situated in the animal facility of Hangzhou Medical College. The experimental protocol was approved by the Hangzhou Medical College Animal Ethics Committee (2022-001). (The study was conducted in accordance with local legislation and institutional requirements.) All mice were subjected to the controlled temperature of 24−26 °C with a 12 h light−dark cycle. They had an *ad libitum* availability of nourishment and hydration. These mice were subjected to random allocation to one of five groups: wild-type (WT), APP/PS1, APP/PS1 + 1 mg/kg Iso, APP/PS1 + 10 mg/kg Iso, and APP/PS1 + 5 mg/kg donepezil. Each group consisted of 10 female mice weighing approximately 30 g and age 10 months. The drugs were dissolved in 1× phosphate-buffered saline (PBS). Intraperitoneal injections were given to the APP/PS1 mice, while the WT and APP/PS1 control groups received isoenergetic quantities of 1× PBS. After one month of drug treatment, the cognitive abilities of all mice were assessed using the Morris water maze (MWM) and novel object recognition (NOR) tests.

Novel Object Recognition. The experimental setup consisted of a square arena measuring 25 × 25 cm, enclosed by four walls measuring 40 cm in height. An overhead video camera was positioned to capture the behavior of the mice. Prior to the experiment, all mice underwent a period of acclimatization in the experimentation chamber to familiarize them with the test environment. On the first day of testing, the arena contained two identical objects, labeled as Object A. These objects were red in color, featuring dimensions of 4.9 cm in diameter and 3 cm in height. The mice were introduced into the arena, and the recording equipment was activated to track their movements. The following parameters were recorded: the frequency the mice engaged with the materials and the duration of exploration within a 2−3 cm range of the objects. The experiments were conducted for 5 min. After a 24 h interval, one of the initial materials (Object A) was substituted with a new object, referred to as Object B. Object B was green in color, with a length of 5.4 cm, a width of 5 cm, and a height of 3 cm. The experiment was again recorded for a period of 5 min. Subsequently, the mice's performance was analyzed. Mice with poor cognitive abilities would exhibit no deviation in their examination of the new and original objects. In contrast, mice with normal cognitive abilities would tend to take additional time to explore the new object.[27]

Morris Water Maze Test. Following the established protocol, the MWM test was used to observe the effect of Iso on improving the learning and memory ability of mice. The MWM apparatus constituted a round reservoir with a cylindrical object measuring 100 cm across and 38 cm in vertical extent. It featured a transportable platform (6 cm in diameter) and four equidistant visual cues on the pool wall. The hydrothermal milieu was maintained at 22−26 °C throughout the scientific inquiry. Prior to the memory task, the mice were habituated to the observational habitat 1 day in advance. The mice were given four consecutive days of training, during which they had to locate a hidden platform fixed beneath the water surface (approximately 1 cm). On the fifth day, a spatial recognition evaluation without the presence of the platform was conducted. The experiments were conducted in the morning, and the temporal period taken by each individual mouse to locate the platform was documented by using an overhead video camera. The mice were placed in a warming cage during the intertrial intervals. This procedure was repeated on days 2, 3, and 4. The average latency across the four-day training sessions was calculated as a measure of the learning ability for each mouse. On the fifth day, the platform was eliminated, and the mice were permitted to freely explore the pool for 60 s in a spatial exploration test. The figure of crossings over the previous platform location and the duration elapsed in each quadrant were documented. The MWM visual surveillance and automated analysis system (VisuTrack) was used for data acquisition and analysis.[27]

Tissue Sample Preparation. All mice were euthanized using sodium pentobarbital (200 mg/kg), and their brains and blood were collected. Half of the brain tissue was fixed in 4% paraformaldehyde solution at 4 °C for 24−48 h. Subsequently, samples were dehydrated on a sucrose gradient, fixed in optimal cutting temperature compound (OCT), and stored at −80 °C for subsequent tissue immunofluorescence assays. The remaining brain tissues were lysed with radio immunoprecipitation assay lysis buffer (RIPA) and used for subsequent experiments.

Immunofluorescence (IF). The brain tissue was embedded in the OCT and subsequently sectioned into 15 μm thick slices utilizing a low-temperature thermostat (CM3050, Leica). These sections were subjected to three washes with 1× PBS, and subsequently, 0.3% Triton X-100 was used for 20 min to make the sections transparent. Following this, the sections were blocked with 10% BSA at room temperature for 1 h. Next, the tissue sections underwent overnight incubation at 4 °C with the primary antibody, which was diluted at a ratio of 1:200 in PBS containing 1% BSA. On the following day, the tissue sections were allowed to equilibrate at room temperature for 30 min, and then the primary antibody was washed out with 1× PBS three times. Sections underwent incubation with the appropriate secondary antibody (diluted at 1:500) for 1 h at 25 °C, while being

https://doi.org/10.1021/acs.jnatprod.3c00894
J. Nat. Prod. XXXX, XXX, XXX−XXX

kept in the dark. After incubation, the sections were washed three times in PBS and excess moisture. Nuclei were counterstained using DAPI from Sigma (D6578) for 2 min. Cerebral images were captured using a Nikon A1 confocal microscope. Each experiment was performed in triplicate.

SOD and MDA Assays. The investigative procedure was performed in compliance with the prescribed guidelines provided by the respective manufacturers. To extract protein samples from brain tissues, a RIPA lysis buffer (Beyotime) was utilized. The levels of SOD and MDA were determined using specific assay kits purchased from Beyotime. For the measurement of the SOD activity, a WST-8 assay was employed. The WST-8 reagent reacts with superoxide anions, which are generated by xanthine oxidase, resulting in the production of a water-soluble formazan dye. The optical density of the formazan dye was quantified at 450 nm by using a suitable microplate reader. To determine the MDA content, a colorimetric response triggered by the reaction between MDA and thiobarbituric acid was employed. This reaction produces a red product that can be quantified by employing a 532 nm filter for measurement. The absorbance was evaluated by using a BIO-RAD680 microplate reader.

Statistical Analysis. Statistical analyses were processed utilizing GraphPad Prism 8.0 software. The findings are reported as the mean ± standard error of the mean from three autonomous experiments. To determine the statistical significance across multiple cohorts, either one-way or two-way analysis of variance (ANOVA) was performed, followed by Tukey's *posthoc* test. The level of statistical significance was set at $P < 0.05$.

■ ASSOCIATED CONTENT

Data Availability Statement

The raw data supporting the conclusions of this article will be made available by the authors upon reasonable requests.

Supporting Information

The Supporting Information is available free of charge at https://pubs.acs.org/doi/10.1021/acs.jnatprod.3c00894.

Details of the table of natural products used for the screening assay and toxicity test of Iso on PC12 cells (PDF)

■ AUTHOR INFORMATION

Corresponding Authors

Xia Zhao − *Affiliated Yongkang First People's Hospital and School of Pharmacy, Hangzhou Medical College, Hangzhou, Zhejiang 311399, China;* orcid.org/0000-0002-7980-8592; Email: xiazhao@hmc.edu.cn

Wei Wang − *Affiliated Yongkang First People's Hospital and School of Pharmacy, Hangzhou Medical College, Hangzhou, Zhejiang 311399, China*; Email: ykoneway2000@126.com

Guang Liang − *Affiliated Yongkang First People's Hospital and School of Pharmacy, Hangzhou Medical College, Hangzhou, Zhejiang 311399, China*; Email: wzmcliangguang@163.com

Authors

Li Xiong − *Affiliated Yongkang First People's Hospital and School of Pharmacy, Hangzhou Medical College, Hangzhou, Zhejiang 311399, China*

Lingyu She − *Key Laboratory of Natural Medicines of the Changbai Mountain, Ministry of Education, Yanbian University, Yanji, Jilin 133002, China*

Jinfeng Sun − *Affiliated Yongkang First People's Hospital and School of Pharmacy, Hangzhou Medical College, Hangzhou, Zhejiang 311399, China; Key Laboratory of Natural Medicines of the Changbai Mountain, Ministry of Education, Yanbian University, Yanji, Jilin 133002, China*

Xiangwei Xu − *Affiliated Yongkang First People's Hospital and School of Pharmacy, Hangzhou Medical College, Hangzhou, Zhejiang 311399, China;* orcid.org/0000-0003-0035-4303

Liwei Li − *Affiliated Yongkang First People's Hospital and School of Pharmacy, Hangzhou Medical College, Hangzhou, Zhejiang 311399, China*

Yuqing Zeng − *Affiliated Yongkang First People's Hospital and School of Pharmacy, Hangzhou Medical College, Hangzhou, Zhejiang 311399, China*

Hao Tang − *Affiliated Yongkang First People's Hospital and School of Pharmacy, Hangzhou Medical College, Hangzhou, Zhejiang 311399, China*

Complete contact information is available at: https://pubs.acs.org/10.1021/acs.jnatprod.3c00894

Funding

This study was supported by the Natural Science Foundation of Zhejiang Province (LQ23H090018 to X.Z. and LTGY23H090001 to W.W.) and Zhejiang Provincial Key Scientific Project (2021C03041 to G.L.).

Notes

The authors declare no competing financial interest.

■ ACKNOWLEDGMENTS

We would like to thank the Hangzhou Medical College for providing the experimental facility to support this research.

■ REFERENCES

(1) Therriault, J.; Zimmer, E. R.; Benedet, A. L.; Pascoal, T. A.; Gauthier, S.; Rosa-Neto, P. *Trends in molecular medicine* **2022**, *28* (9), 726−741.

(2) Khan, S.; Barve, K. H.; Kumar, M. S. *Current neuropharmacology* **2020**, *18* (11), 1106−1125.

(3) Yu, T. W.; Lane, H. Y.; Lin, C. H. Novel Therapeutic Approaches for Alzheimer's Disease: An Updated Review. *International Journal of Molecular Sciences* **2021**, *22* (15).

(4) Ballard, C.; Gauthier, S.; Corbett, A.; Brayne, C.; Aarsland, D.; Jones, E. *Lancet (London, England)* **2011**, *377* (9770), 1019−31.

(5) Zhou, H.; Gong, Y.; Liu, Y.; Huang, A.; Zhu, X.; Liu, J.; Yuan, G.; Zhang, L.; Wei, J. A.; Liu, J. *Biomaterials* **2020**, *237*, 119822.

(6) Gan, Q.; Yao, H.; Na, H.; Ballance, H.; Tao, Q.; Leung, L.; Tian, H.; Zhu, H.; Wolozin, B.; Qiu, W. Q. *Journal of Alzheimer's Disease* **2019**, *70* (4), 1025−1040.

(7) Tolar, M.; Hey, J.; Power, A.; Abushakra, S. Neurotoxic Soluble Amyloid Oligomers Drive Alzheimer's Pathogenesis and Represent a Clinically Validated Target for Slowing Disease Progression. *International Journal of Molecular Sciences* **2021**, *22* (12), 6355.

(8) Leng, F.; Edison, P. *Nature Reviews. Neurology* **2021**, *17* (3), 157−172.

(9) Megha, K. B.; Joseph, X.; Akhil, V.; Mohanan, P. V. *Phytomedicine: international journal of phytotherapy and phytopharmacology* **2021**, *91*, 153712.

(10) Agrawal, I.; Jha, S. *Frontiers in aging neuroscience* **2020**, *12*, 252.

(11) Tong, B. C.; Wu, A. J.; Li, M.; Cheung, K. H. *Biochimica et biophysica acta. Molecular cell research* **2018**, *1865* (11), 1745−1760.

(12) Naseri, N. N.; Wang, H.; Guo, J.; Sharma, M.; Luo, W. *Neuroscience letters* **2019**, *705*, 183−194.

(13) Shen, X.; Chen, H.; Zhang, H.; Luo, L.; Wen, T.; Liu, L.; Hu, Q.; Wang, L. *International immunopharmacology* **2023**, *124*, 110965.

(14) Zhang, H.; Zheng, Y. *Acta Academiae Medicinae Sinicae* **2019**, *41* (5), 702−708.

(15) Cline, E. N.; Bicca, M. A.; Viola, K. L.; Klein, W. L. *Journal of Alzheimer's disease* **2018**, *64* (s1), S567−s610.

(16) Cheignon, C.; Tomas, M.; Bonnefont-Rousselot, D.; Faller, P.; Hureau, C.; Collin, F. *Redox biology* **2018**, *14*, 450−464.
(17) Zhong, B. R.; Zhou, G. F.; Song, L.; Wen, Q. X.; Deng, X. J.; Ma, Y. L.; Hu, L. T.; Chen, G. J. *FASEB journal: official publication of the Federation of American Societies for Experimental Biology* **2021**, *35* (5), No. e21445.
(18) Yue, J.; López, J. M. Understanding MAPK Signaling Pathways in Apoptosis. *International journal of molecular sciences* **2020**, *21* (7), 2346.
(19) Kheiri, G.; Dolatshahi, M.; Rahmani, F.; Rezaei, N. *Reviews in the neurosciences* **2018**, *30* (1), 9−30.
(20) DeTure, M. A.; Dickson, D. W. *Molecular neurodegeneration* **2019**, *14* (1), 32.
(21) Mangalmurti, A.; Lukens, J. R. *Current opinion in neurobiology* **2022**, *75*, 102575.
(22) Han, C.; Yang, Y.; Guan, Q.; Zhang, X.; Shen, H.; Sheng, Y.; Wang, J.; Zhou, X.; Li, W.; Guo, L.; Jiao, Q. *Journal of cellular and molecular medicine* **2020**, *24* (14), 8078−8090.
(23) Kwak, A. W.; Park, J. W.; Lee, S. O.; Lee, J. Y.; Seo, J. H.; Yoon, G.; Lee, M. H.; Choi, J. S.; Shim, J. H. *Phytomedicine: international journal of phytotherapy and phytopharmacology* **2022**, *105*, 154383.
(24) Park, J. H.; Kim, M. J.; Kim, W. J.; Kwon, K. D.; Ha, K. T.; Choi, B. T.; Lee, S. Y.; Shin, H. K. *Cancer letters* **2020**, *478*, 71−81.
(25) Chen, Y. Y.; Liu, Q. P.; An, P.; Jia, M.; Luan, X.; Tang, J. Y.; Zhang, H. *Phytomedicine: international journal of phytotherapy and phytopharmacology* **2022**, *95*, 153883.
(26) Wu, J. J.; Yang, Y.; Wan, Y.; Xia, J.; Xu, J. F.; Zhang, L.; Liu, D.; Chen, L.; Tang, F.; Ao, H.; Peng, C. *Biomedicine & pharmacotherapy* **2022**, *152*, 113207.
(27) She, L.; Xiong, L.; Li, L.; Zhang, J.; Sun, J.; Wu, H.; Ren, J.; Wang, W.; Zhao, X.; Liang, G. *Biomedicine & pharmacotherapy* **2023**, *158*, 114192.
(28) Shin, S. J.; Jeong, Y.; Jeon, S. G.; Kim, S.; Lee, S. K.; Choi, H. S.; Im, C. S.; Kim, S. H.; Kim, S. H.; Park, J. H.; Kim, J. I.; Kim, J. J.; Moon, M. *Neurochemistry international* **2018**, *121*, 114−124.
(29) Park, H. J.; Lee, K.; Heo, H.; Lee, M.; Kim, J. W.; Whang, W. W.; Kwon, Y. K.; Kwon, H. *Phytotherapy research: PTR* **2008**, *22* (10), 1324−9.
(30) Xu, M.; Yan, T.; Fan, K.; Wang, M.; Qi, Y.; Xiao, F.; Bi, K.; Jia, Y. *Journal of ethnopharmacology* **2019**, *237*, 354−365.
(31) Kumari, S.; Dhapola, R.; Reddy, D. H. Apoptosis in Alzheimer's disease: insight into the signaling pathways and therapeutic avenues. *Apoptosis* **2023**, *28*, 943.
(32) He, B.; Chen, W.; Zeng, J.; Tong, W.; Zheng, P. *Journal of cellular physiology* **2020**, *235* (1), 480−493.
(33) Chiu, Y. J.; Hsieh, Y. H.; Lin, T. H.; Lee, G. C.; Hsieh-Li, H. M.; Sun, Y. C.; Chen, C. M.; Chang, K. H.; Lee-Chen, G. J. *Neurochemistry international* **2019**, *125*, 175−186.
(34) Wang, Q.; Jiang, H.; Wang, L.; Yi, H.; Li, Z.; Liu, R. *Journal of Alzheimer's disease* **2019**, *72* (1), 199−214.
(35) Zhang, Y.; Zhao, Y.; Zhang, L.; Yu, W.; Wang, Y.; Chang, W. *Frontiers in cellular neuroscience* **2019**, *13*, 339.
(36) Lauritzen, I.; Pardossi-Piquard, R.; Bourgeois, A.; Pagnotta, S.; Biferi, M. G.; Barkats, M.; Lacor, P.; Klein, W.; Bauer, C.; Checler, F. *Acta neuropathologica* **2016**, *132* (2), 257−276.
(37) Zhao, X.; Huang, X.; Yang, C.; Jiang, Y.; Zhou, W.; Zheng, W. Artemisinin Attenuates Amyloid-Induced Brain Inflammation and Memory Impairments by Modulating TLR4/NF-κB Signaling. *International journal of molecular sciences* **2022**, *23* (11).
(38) Durairajan, S. S.; Yuan, Q.; Xie, L.; Chan, W. S.; Kum, W. F.; Koo, I.; Liu, C.; Song, Y.; Huang, J. D.; Klein, W. L.; Li, M. *Neurochemistry international* **2008**, *52* (4−5), 741−50.

https://doi.org/10.1021/acs.jnatprod.3c00894
J. Nat. Prod. XXXX, XXX, XXX−XXX